ANTIOXIDANTS & REDOX SIGNALING
Volume 9, Number 1, 2007

Original Research Communication

Hypertension Caused by Transgenic Overexpression of Rac1

HAMDY H. HASSANAIN,[1,2] DAVID GREGG,[3] MARIA LUISA MARCELO,[4] JAY L. ZWEIER,[2] HERALDO P. SOUZA,[5] BALAKRISHNAN SELVAKUMAR,[6] QI MA,[8] MOUSTAFA MOUSTAFA-BAYOUMI,[7] PHILLIP F. BINKLEY,[2] NICHOLAS A. FLAVAHAN,[2] MARIANA MORRIS,[4] CHUNMING DONG,[6] and PASCAL J. GOLDSCHMIDT–CLERMONT[8]

ABSTRACT

Reactive oxygen species, including superoxide, are important mediators of the pathophysiology of hypertension. In the vasculature, superoxide antagonizes nitric oxide ($NO^{\bullet}$), resulting in increased vascular tone. The GTP binding protein Rac regulates a wide variety of cellular functions, including the activation of NADPH oxidase, the major source of $O_2^{\bullet-}$ in the blood vessel wall. An hypothesis is that Rac1 may act as an important regulator of vascular $O_2^{\bullet-}$ production, contributing to the balance between $O_2^{\bullet-}$ and $NO^{\bullet}$ and maintaining consequent homeostasis of blood pressure. To alter the activity of vascular NADPH oxidase, the authors developed a transgenic animal model that overexpresses the human cDNA of the constitutively active mutant of Rac1 (RacCA) in smooth muscle cells using the smooth muscle α-actin promoter. The RacCA transgenic had excessive amounts of $O_2^{\bullet-}$ in the vessel wall that, which led to heightened production of peroxynitrite, as detected by increased protein nitration and reduced $NO^{\bullet}$ levels. RacCA mice developed moderate hypertension, which was corrected by *N*-acetyl-L-cysteine (NAC). RacCA transgenic mice also developed left ventricular hypertrophy as a secondary effect of pressure overload. The data suggest that Rac1 is a critical regulator of the redox state of blood vessels and homeostasis of blood pressure. *Antioxid. Redox Signal.* 9, 91–100.

INTRODUCTION

THE PHYSIOLOGY OF BLOOD pressure is determined by cardiac output and vascular resistance to blood flow, both of which are influenced by a wide variety of physiologic systems. An important pathway is activated by angiotensin II and recruits a vascular NADPH (6, 18, 31) oxidase activity (8, 25). NADPH oxidase, whose activity is regulated by the small guanyl nucleotide binding protein Rac, represents the principal source of superoxide in blood vessels (15, 30). Nitric oxide ($NO^{\bullet}$), produced by $NO^{\bullet}$ synthase, mediates its physiological effects mainly via activation of a cytoplasmic form of guanylyl cyclase and the production of cGMP, which in turn activates G-kinase (3). The maintenance of physiological blood pressures corresponds to a balancing act between $NO^{\bullet}$ (vasodilator) and $O_2^{\bullet-}$ (vasoconstrictor) that has been disrupted, and the cause of such disruption could be the altered production of $O_2^{\bullet-}$ (2, 3, 31). Nitric oxide and superoxide swiftly react with each other to produce peroxynitrite ($ONOO^-$) in a fashion that negates their individual effects on the vasculature but leads to the production of potentially toxic substances for vascular cells (7, 14, 21, 33). The loss of $NO^{\bullet}$ to peroxynitrite could impair the ability of resistance vessels to become di-

[1]Department of Anesthesiology and [2]Dorothy M. Davis Heart and Lung Institute, The Ohio State University, Columbus, Ohio.
[3]Medical University of South Carolina, Charleston, South Carolina.
[4]Department of Pharmacology and Toxicology, Wright State University, Dayton, Ohio.
[5]Disciplina de Emergencias Clinicas, Faculdade de Medicina da Universidade de Sao Paulo, Brazil.
[6]Division of Cardiology, Duke University, Durham, North Carolina.
[7]Department of Kinesiology and Health Promotion, California State Polytechnic University, Pomona, California.
[8] University of Miami Miller School of Medicine, Miami, Florida.

lated leading to a more rigid vessel that is hypertensive in nature.

The small GTP binding protein, Rac, is the point of convergence for multiple pathways leading to production of $O_2^{\bullet-}$ through NADPH oxidase (23). To study the effect of Rac activation on blood pressure, we engineered transgenic mice overexpressing the cDNA of a constitutively active mutant of human Rac1 (RacCA) gene in smooth muscle cells (SMCs), under the control of mouse smooth muscle α-actin (SMA) promoter. Our hypothesis is that Rac1 may act as an important regulator of vascular $O_2^{\bullet-}$ production, contributing to the balance between $O_2^{\bullet-}$ and $NO^{\bullet}$ and maintaining consequent homeostasis of blood pressure.

METHODS

Generation of transgenic mice

The cDNA coding for RacCA with glycine 12 to valine substitution and a myc-tag (a gift from Alan Hall) was subcloned into the EcoRI site of Bluescript II KS+ to create new restriction sites. Smp8 plasmid was cut with Xho1, and the blunt end was produced by filling and then cutting again with Kpn1. The cDNA of RacCA, including its polyadenylation tail, was cloned within the blunt Xho1 and Kpn1 ends of the Smp-8 plasmid that contained a 3.6 kb segment of the 5′-region of SMA promoter. The SMA promoter was used to induce selective overexpression of RacCA in SMCs. The Sph1/Kpn1 fragment of this plasmid was isolated and microinjected into mouse fertilized eggs of FVB/N females, as described previously (10). Single-cell embryos derived from superovulated FVB/N females were used for the microinjection procedure. Surviving microinjected embryos were implanted into pseudopregnant FVB/N foster mothers. Founder mice were identified using Southern blot analysis. Founder mice with the highest expression of RacCA were used to establish the transgenic line. All the experiments were performed with male heterozygous RacCA transgenic mice (4- to 5-month-old) with age matched nontransgenic littermates.

Southern blot analysis

Genomic DNA was isolated from mouse tail clips and 20 μg from each sample was digested with EcoRI to release the human RacCA cDNA, and then separated by electrophoresis on a 0.8% agarose gel. Gel electrophoresis was conducted at 0.5 V/cm for 24 h in the buffer containing 30 mmol/L NaOH and 2 mmol/L EDTA. The gels were then neutralized in 1 *M* Tris, pH 7.4, and 1.5 *M* NaCl, and DNA was transferred to Hybond N^+ nylon membrane (Amersham Biosciences, Piscataway, NJ) by capillary blotting. The cDNA corresponding to RacCA was labeled with α-^{32}P-dCTP by *rediPrime* DNA Labeling Kit (Amersham Biosciences) and hybridized to the membrane following the manufacturer's protocols. Washes were performed with 2X SSC once and 0.1X SSC twice. Finally, radiolabeled human RacCA cDNA bands were detected on X-ray film to confirm the proper recombination of the human RacCA gene into the mouse genome.

Reverse transcriptase–polymerase chain reaction (RT–CR)

Tissues isolated from mice were immediately frozen in liquid nitrogen (N_2). The frozen tissues were ground in liquid N_2 by mortar and pestle. Total cellular RNA was extracted using TRIzol reagent (Invitrogen, Carlsbad, CA) and the integrity of total RNA and genomic DNA were checked on agarose gel. The first-strand cDNA was synthesized utilizing Superscript II (Gibco-BRL, Carlsbad, CA), then amplified using Taq-DNA polymerase (Gibco BRL) with 35 cycles of denaturation (94°C, 45 s), primer annealing (55°C, 30 s), and extension (72°C, 2 min). The cDNA was amplified using specific primers for RacCA cDNA. The first primer, the c-myc primer, recognized the c-myc epitope sequence that attached to 5′ end of the cDNA (GAGCAGAAGCTGATCT CCGAGGAG). The reverse primer was derived from the 3′ end of the RacCA cDNA (5′-TTACAACA GCAG GCA TTTTCTCTT-3′).

Western blot analysis

Aortas isolated from mice were immediately frozen in liquid nitrogen (N_2). The frozen tissues were ground in liquid N_2 by mortar and pestle and resuspended in RIPA buffer (Upstate Biotechnology, Charlottesville, VA). Aortic extracts from Rac CA and control mice (n = 8) were separated on SDS-polyacrylamide (4–20%) gels and transferred to nitrocellulose membrane (Hybond ECL, Amersham International). Membranes were blocked in 5% BSA and subsequently incubated in anti-Rac, anti-Myc, anti-nitro tyrosine or anti-eNOS antibody, according to standard protocols (Upstate Biotechnology). We used an agarose conjugated monoclonal anti-Rac antibody (Upstate Biotechnology) for immunoprecipitation. Cultured wild-type SMCs transduced with adenovirus specifying RacCA (400 MOI) with identical c-Myc tag served as positive control. Proteins were detected via enhanced chemiluminescence using the Supersignal Chemiluminescent Substrate Kit (Pierce, Rockford, IL) for 5 min, followed by exposure to Kodak Biomax ML film (Sigma, St. Louis, MO).

P21-activated kinase (PAK) binding assay

Rac1 activity was determined using a commercially available kit (Upstate Biotechnology). Aortic lysates from RacCA and control mice (n = 8) were incubated with either GST alone or GST-PBD (p21-binding domain) fusion protein bound to glutathione coupled to Sepharose beads at 4°C for 30 min. Bound (activated) Rac was separated by repetitive centrifugation and washing. After the specimens were boiled in LAEMMLI buffer (62.5 m*M* Tris-HCl, pH 6.8, 2% SDS, 25% glycerol, 0.01% Bromophenol Blue), they were subjected to SDS-PAGE, and Rac was quantified by Western blot analysis using Rac 1 antibody. Nontransgenic lysate diluted by 10 times and incubated with GTPγS (nonhydrolyzable GTP) prior to precipitation served as positive control.

Immunohistochemistry

The aortas from transgenic and nontransgenic litter mates (n = 8) were divided into two segments, one segment was snap-frozen in OCT (Redding, CA), and the other segment was fixed in 10% neutral buffered formalin. Immunohistochemistry was

performed on 4 micron sections from formalin-fixed and paraffin-embedded tissue using Vector's ABC kit (Vector, Los Angeles, CA) according to the manufacturer's instructions to analyze the expression for nitrotyrosine and eNOS.

Superoxide detection by EPR spectroscopy in intact vessels

RacCA transgenic mice and matched control littermates (n = 7) were sacrificed by intraperitoneal injection of sodium pentobarbital (100 mg/kg). Thoracic aortas were removed, freed from periadventital and loose connective tissue, and immediately incubated with the spin trap 5,5′-dimethyl-pyrroline-N-oxide (DMPO, 50 m*M*), diluted in buffer (PBS plus EDTA 0.01 m*M*, pH = 7.40, final volume 0.6 ml) at 37°C for 30 min. After this period, the solution was removed and frozen in liquid nitrogen, the vessels were placed in a similar solution, only where diethyldithiocarbamate (DETC, 1.0 m*M*) was added (34, 36). The aortic rings were maintained in this solution at 37°C, for 30 min, after which the solution was frozen in liquid nitrogen and the vessels transferred to a solution where DETC 1.0 m*M* and a membrane-permeant superoxide dismutase mimetic (SODm, M40403, 20 μ*M*) were added (5, 27). After 30 min, the solution was frozen and the vessels dried on filter paper at 60°C for 2 h. The frozen samples were thawed and EPR spectra were recorded in a quartz flat cell at room temperature (23°C) with a Bruker ER 300 spectrometer (Bruker, Billerica, MA) operating at X-band with a TM_{110} cavity using a modulation frequency of 100 kHz, modulation amplitude of 0.5 G, microwave power of 20 milliwatts, and microwave frequency of 9.78 GHz as described (35). The microwave frequency and magnetic field were precisely measured using an EIP 575 microwave frequency counter and Bruker ER 035 NMR gaussmeter. Ten serial 60 s-acquisitions with 80-Gauss sweep were accumulated to obtain the final spectrum. Four spectra were acquired from each sample. Results were expressed as arbitrary units, which were obtained measuring the amplitude and intensity of the spectrum, and subtracting the amplitude of the background spectra.

Measurement of ROS and NO level in the vessel wall

Fifty-μm aortic sections were obtained from RacCA (n = 12) and nontransgenic (n = 16) aortas incubated with dihyroethidium (DHE) for superoxide staining. In another experiment, aortic sections from RacCA mice (n = 10) were incubated with gp91ds-tat, a specific inhibitor for NADPH oxidase before DHE staining as described in the manufacture's protocol (Molecular Probes, Eugene, OR). Nitric oxide was assessed in aortic sections from RacCA (n = 16) and control mice (n = 16) using 4,5-diaminofluorescein diacetate (DAF-2 DA) for $NO^{\bullet}$ staining for 15 min at 37°C and imaged with confocal microscopy following manufacture's instructions (Molecular Probes).

TaqMan real-time RT–PCR (TRT–PCR)

Superoxide dismutase isoforms were assessed in the aortas of RacCA transgenic mice (n = 8) and matched control littermates (n = 6). RNA was isolated from aortas using a QIAGEN kit (QIAGEN, Valencia, CA) and cDNA was synthesized from RNA using Superscript II (Gibco BRL), as mentioned above. Taqman probes and primers for Cu/Zn SOD, MnSOD, and ecSOD were designed using primer 3 software (MIT). TaqMan reactions were carried out using primers (400 n*M*) corresponding to individual SODs, or primers for an internal standard (18S-RNA, 100 n*M*), relevant probes (4 μ*M*), 12.5 μl of TaqMan master mix for a final sample volume of 25 μl. The PCR was run at standard conditions in the AB1Prism sequence detector system. The sequence of the primers and probes are: (a) Cu/Zn SOD forward: 5′-TGTGGAGTGATTGGGATTG-3′, reverse primer is 5′-TGGTTTGAGGGTA GCAGTTG-3′, florescence probe 5′-(FAM)-CGCAGTAAACAT TCCCTGT-GTGG-3′ (TAMRA); (b) extracellular SOD forward: 5′-AAGAGGAGGAGGC AGCAA-3′, reverse primer: 5′-GTCAGCAAATGGAGGAAG-3′ and fluorescent probe 5′-(FAM)-TACCACAAGGGACAGCCAAGC-3′ (TAMRA); (c) Mn SOD forward: 5′-GAGTTGCTGGAGGCTATCAA-3′, reverse primer: 5′-CGACCTTGCTCC TTATT GAA-3′, and fluorescent probe 5′-(FAM)-GCGTGACTTTGGGTC-TTTTGAGAA-3′ (TAMRA). The mRNA levels for catalase, glutathione peroxidase (GPX), and glutathione reductase (GR) were quantitatively determined in the aortas of RacCA transgenic mice (n = 7) and matched control littermates (n = 7) using SYBR-green real-time RT–PCR. In 96-well plates, 12.5 μl SYBER-green master mix was added to 12.5 μl of cDNA (1% of the amount of cDNA derived from 0.5 μg mRNA) and 300 n*M* of forward and reverse primers in water. The PCR was run at standard conditions in the AB1Prism sequence detector system. The sequence of the primers and probes are: (a) catalase forward: 5′-ATGGCTTTTGACCCAAGCAA-3′, reverse primer is 5′-CGGCC CTGAAGCTTTTTGT-3′; (b) GPX forward: 5′-GCGGCCCTGGCATTG-3′, reverse primer: 5′-GGACCAGCGCC CATCTG-3′; and (c) GR forward: 5′-CCGCTCCACACATCC TGAT-3′, reverse primer: 5′-AA-GAAGCCATCGCTGGTGAT-3′. After PCR amplification, dissociation curves were constructed to confirm formation of the intended PCR products. Expression levels of target genes were related to the expression levels of 18S RNA. Relative expression levels were calculated as described in Applied Biosystems User Bulletin (Applied Biosystems, Foster City, CA).

Measurements of SOD activity

Aortas from transgenic (n = 6) and nontransgenic littermates (n = 6) were dissected, perfused with cold saline buffer to remove blood contaminants, and snap-frozen in liquid N_2. The frozen tissue was pulverized in liquid N_2, suspended in lysis buffer containing protease inhibitors, then extracted further using tissue sonication. SOD activity was measured using the Bioxytech kit (R & D Systems, Minneapolis, MN) according to the manufacturer's instructions.

Blood pressure and heart rate measurements

RacCA transgenic males (4- to 5-month-old; n = 8) and age matching control littermates (n = 8) were used to monitor blood pressure and heart rate. For chronic cardiovascular monitoring, mice were outfitted with carotid arterial catheters (micrenathane, Braintree Scientific, Braintree, MA). Animals were

anesthetized using a 5:2 ketamine/xylazine mixture and the surgery was conducted as previously described (16). The catheter was protected by a stainless steel spring and connected to a swivel located on top of the cage. The tether and swivel system allowed the animal to move freely while protecting the catheter. A continuous infusion of 60 U/ml of heparinized saline (25 µl/h) was used to maintain catheter patency. By 3–4 days postsurgery, the mice displayed a stabilized pattern of behavior and food and water intake. Arterial blood pressure (MAP ± SEM) and heart rate (HR) were measured continuously for 4 days via external carotid artery across the night/day cycle using a data acquisition system (Biopac, Santa Barbara, CA) with a sampling rate of 100 Hz. Circadian rhythm analysis was obtained by converting data to text files for plotting and analysis using Circadia program, specific for biological rhythms analysis (Behavioral Cybernetics, Boston, MA). MAP and HR daily rhythms were quantified by calculating ratios of mean values in the dark and light periods. The data was then smoothed using a 30-min moving average, followed by average waveform calculations. For the administration of *N*-acetylcysteine (NAC), the protocol included 4 days of baseline cardiovascular measurements, 4 days of chronic arterial infusion with 0.5 g/kg body weight/day of NAC, and 4 days of recovery.

Echocardiography

Echocardiographic measurement of left ventricular mass was performed on RacCA transgenic (n = 7) and nontransgenic matched controls (n = 7). Mice were anesthetized with isofluorane by inhalation. The chest of the mouse was shaved. Two-dimensional and M-mode echocardiographic studies were performed with a commercially available 15-MHz linear array transducer system (Sonos 5500, Hewlett Packard, Loveland, CO).

Statistical analysis

Data are presented as the mean ± SEM . The data were analyzed with ANOVA by means of InStat 2.01 (GraphPad Software, San Diego, CA) to compare differences between RacCA and control mice. A *p value of ≤ 0.05 was considered statistically significant.

RESULTS

Generation of transgenic mice

We engineered a transgenic mouse overexpressing the constitutively active mutant of the human Rac1 gene (RacCA) in FVB/N mice, using mouse SMA promoter. Three transgenic founders were identified using Southern blot analysis of tail genomic DNA, and they were used to establish three stable heterozygous transgenic lines by breeding with nontransgenic FVB/N mates. All three transgenic lines displayed a similar phenotype. Data obtained from the founder line confirmed having the highest number of human Rac-CA gene copies are reported here. Southern blot analysis of genomic DNA from tails of F1 founder offspring indicated that nearly 50% were transgenic (Fig. 1A).

Expression of RacCA in transgenic mice

To detect expression of RacCA in transgenic mice, various tissues were analyzed by RT–PCR using primers that selectively recognize the transgene. RT–PCR analysis revealed selective transcription of RacCA in smooth muscle, including blood vessels, spleen, and intestine (Fig. 1B). Kidney tissue was also positive for RacCA, as the mesangial cells of glomeruli express SMA (1). The transgene was not detected in wild-type FVB/N mice (data not shown) nor in organs of transgenic mice that express little SMA, including the heart, liver, and brain (Fig. 1B).

We have previously shown that RacCA exclusively localized in the SMCs of transgenic aortas but not in control aortas using IHC (17). To further determine RacCA expression in the vessel wall of transgenic aortas, we performed immunoprecipitation (IP) using anti-Rac antibody to precipitate aor-

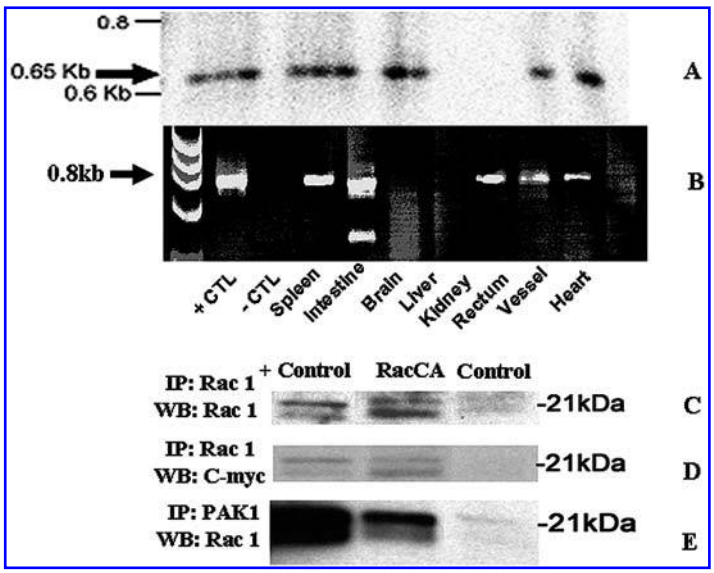

FIG. 1. RacCA overexpression in transgenic mice. Southern blot analysis of tail clips from F1 RacCA mice shows the presence of RacCA transgene. *Arrow* indicates human RacCA (0.65 kb) (**A**). RT–PCR analysis of mRNA isolated from various tissues of RacCA transgenic mice shows selective RacCA overexpression in tissues that express smooth muscle α-actin as indicated in the figure (**B**), the positive control is RacCA cDNA. Immunoprecipitation (IP) for Rac1 followed by Western blot (WB) using anti-Rac1 (**C**) and anti-cMyc (**D**) antibodies. Cultured wild-type SMCs transduced with adenovirus specifying RacCA with identical c-Myc tag served as positive control (**C** and **D**). *In vivo* Rac activation was assessed by affinity precipitation (ppt) for PAK1 followed by Western blotting for Rac1 (**E**). Nontransgenic lysate incubated with GTPγS (nonhydrolyzable GTP) prior to precipitation served as positive control.

tic lysates, followed by blotting with anti-Rac and anti-Myc antibodies that recognize total Rac (endogenous + RacCA) and RacCA-specific protein expression, respectively. Total Rac protein expression was increased by 3.5-fold in RacCA aortas, as compared with their wild-type counterparts (Fig. 1C), whereas RacCA expression was exclusively detected in RacCA aortas (Fig. 1D). We then studied Rac activation using a PAK binding assay that allowed for the detection of endogenous Rac bound to GTP. As shown in Fig. 1E, the amount of Rac-GTP in RacCA aortas was increased by about 16.90-fold compared to wild-type aortas.

Increased ROS activity in RacCA aortas

We used EPR spectroscopy to assess superoxide in intact vessels of RacCA as compare to control littermates. The aortas from wild type or transgenic mice did not show any detectable EPR signal under basal conditions (Fig. 2A, A). This lack of signal does not preclude radical generation, but indicates that levels are below detection. To further enhance the ability to detect superoxide generation, aortas were incubated with DETC to inhibit endogenous SOD (5). Under these conditions, prominent quartet signals, characteristic of DMPO-hydroxyl adduct formation were observed (Fig. 2A, B). This signal is derived from superoxide, since it is completely abolished by a specific membrane-permeant SOD mimetic (Fig. 2A, C). With inhibition of SOD, it is clear that aortas from transgenic mice produce more superoxide than those from wild-type mice (Fig. 2A, A, B, C). Figure 2B shows quantitation of spectra obtained from aortas from wild type and transgenic mice.

To examine the stimulatory effect of RacCA on NADPH oxidase activation, we examined superoxide production in 50 μm aortic rings obtained from transgenic RacCA mice and control littermates using DHE, which reacts with $O_2^{\bullet -}$ to form the fluorescent product ethidium. Ethidial fluorescence levels were increased 18% in transgenic aortas (Fig. 2D) compared to controls (Fig. 2C). The observed fluorescence was quenched by SOD mimetic M40403 (27). After incubation with gp91ds-tat, a specific inhibitor for NADPH oxidase, $O_2^{\bullet -}$ production was decreased 49% (Fig. 2E), indicating that excessive NADPH oxidase activation in RacCA mice is responsible for ROS overproduction.

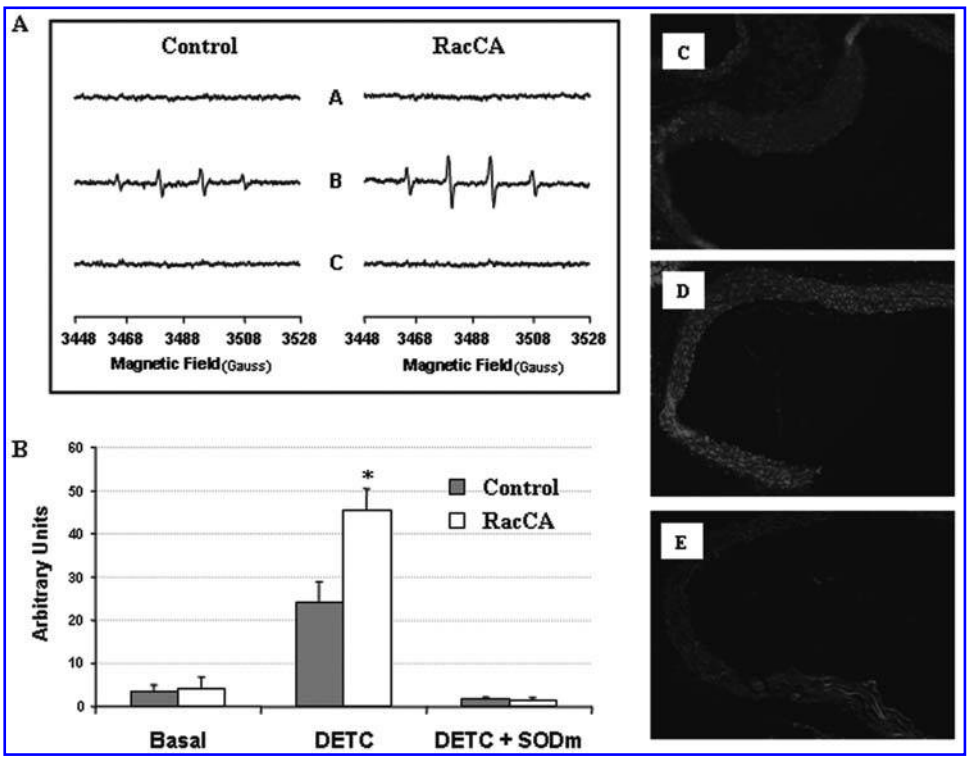

FIG. 2. Increased superoxide production in RacCA aortas. (**A**): EPR spectra of aortas from wild type and transgenic animals. Under basal conditions, aortas from wild type or transgenic mice did not show any detectable EPR signals (*line A*). Prior incubation with DETC, to inhibit SOD, reveals that superoxide generation is higher in the transgenic mouse aortas (*line B*). The observed signals are derived from superoxide, since they are completely abolished by a membrane-permeant SOD mimetic (*line C*). (**B**): quantitation of spectra obtained from aortas from wild type and transgenic animals. When aortas were previously incubated with DETC to inhibit endogenous SOD, a difference in superoxide generation by aortas from wild type and transgenic animals was detected. *$p < 0.05$, transgenic vs. wild type, when incubated with DETC ($n = 7$, each group). (**C, D, E**): DHE staining: basal level $O_2^{\bullet -}$ generation in a wild-type aorta (**C**). RacCA aorta displays a marked increase in $O_2^{\bullet -}$ generation (**D**), which is completely abolished by the NADPH-oxidase-specific inhibiting peptide gp91-ds-tat (**E**). DHE intensity was quantified as relative fluorescence units in aortic sections from NT ($n = 16$), RacCA ($n = 12$), and RacCA + gp91-ds-tat ($n = 10$) (**C**, **D**, **E**).

Renin activity in RacCA mice

Renin activity serves as the rate-limiting element in the control of blood pressure by the RAS system. To determine whether the effect of RacCA on blood pressure might be partly mediated through an increase in renin production, we measured the plasma renin activity in transgenic mice as compared to matched control littermates. Renin activity was defined as the amount of angiotensin I generated from 1 ml plasma per hour. We found that transgenic mice displayed a trend toward less renin activity than control mice (19 ± 7 for wild-type versus 11 ± 4 for RacCA mice).

Increased antioxidant activities in RacCA aortas

To determine whether excess $O_2^{\bullet -}$ affected enzymes that participated in maintaining the redox homeostasis of the cell, we examined whether SOD isoforms, enzymes that scavenge $O_2^{\bullet -}$ anion to covert it to H_2O_2, were upregulated in transgenic aortas. TRT–PCR was performed to quantitate the mRNA levels of the three mammalian isoforms of SOD: Cu/ZnSOD, MnSOD, and ecSOD. Transcription of all three SOD isoforms was markedly upregulated in RacCA aortic tissues relative to nontransgenic aortas, with MnSOD showing the largest increase (4.8-fold) (Fig. 3A). We also measured other key enzymes involved in the antioxidant system in RacCA aortic tissues, including catalase, glutathione peroxidase, and glutathione reductase, and found significant increase in these enzymes, with catalase showing the largest increase (more than fourfold) (Fig. 3B). We then measured total SOD activity in the aortas of matched transgenic and control mice. RacCA overexpression led to a 3.8-fold increase in SOD activity in the transgenic aortic tissues (Fig. 3C).

Decreased NO$^{\bullet}$ level and NO$^{\bullet}$ metabolites in RacCA aortas

Since RacCA aortas displayed increased $O_2^{\bullet -}$ production, we expected that the level of NO$^{\bullet}$ might be decreased in these vessels due to the consumption of NO$^{\bullet}$ by excessive $O_2^{\bullet -}$ Using a fluorescent membrane-permeable marker, DAF-2 DA, we demonstrated that the level of NO$^{\bullet}$ was indeed decreased by 59% in the aortas of RacCA mice (Fig. 4A, B, and C).

Protein nitration in transgenic mice

To determine whether decreased NO$^{\bullet}$ was due to increase NO$^{\bullet}$ consumption or decreased NO$^{\bullet}$ production, or both, we studied protein nitration. Protein nitration serves as a marker for a rapid reaction between $O_2^{\bullet -}$ and NO$^{\bullet}$ to form the highly reactive intermediate peroxynitrite ($OONO^-$). Nitrated proteins were detected by Western blot analysis of aortic extracts and IHC in 4 μm aortic sections using anti-nitrotyrosine antibody. The number and intensity of bands that reacted with the anti-nitrotyrosine antibody were increased in RacCA mice and more nitration was detected in SMCs of RacCA aortas as compared to controls (Fig. 5A, B, and C).

We also studied eNOS expression by IHC and Western blot analysis. Both techniques revealed comparable levels of eNOS expression in RacCA and control aortas (Fig. 5D, E, and F). Thus, despite the reduced NO$^{\bullet}$ bioavailability, eNOS expression does not seem to respond, at least at the tissue protein level, to RacCA overexpression.

Elevated blood pressure in RacCA mice

We measured blood pressure in RacCA mice and control littermates to determine if the excessive $O_2^{\bullet -}$ and decreased NO$^{\bullet}$ in RacCA aortas resulted in elevated blood pressure. Continuous monitoring of blood pressure and heart rate in conscious, nonstressed mice was performed by cannulation of the external carotid arteries of male transgenic (4–5 months) and matched control littermates (as described in the methods). Mean arterial pressure (MAP) of RacCA mice was significantly and consistently higher across the day/night cycle compared to the nontransgenic controls (Fig. 6A). The MAP of transgenic mice fluctuated around 131 mm Hg, while the nontransgenic MAP was stable around 108 mm Hg. In addition, there was no significant difference in HR between transgenic and nontransgenic mice (Fig. 6B). In previous experiments we found no significant differences in the MAP

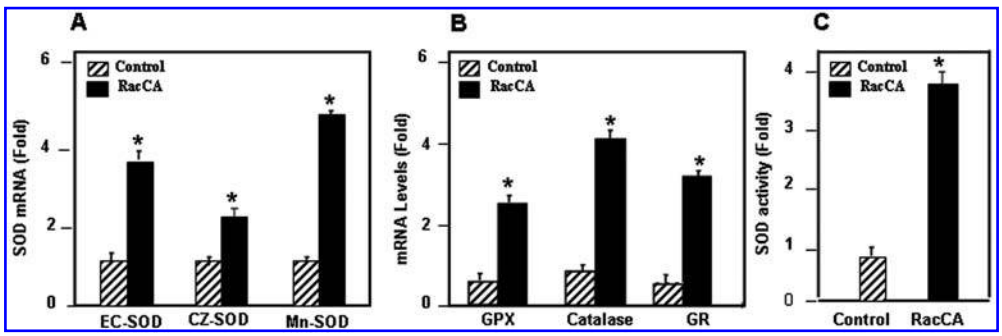

FIG. 3. Increased antioxidants in RacCA mice. TaqMan RT–PCR analysis of SOD isoforms shows increased expression of SOD enzymes in RacCA aortas, with MnSOD displaying the largest increase (**A**). SYBR-green real-time RT–PCR analysis of glutathione peroxidase (GPx), catalase, and glutathione reductase (GR) also show increased expression in RacCA aortas relative to wild-type vessels (**B**). A 3.8-fold increase in SOD activity is detected in RacCA aortas as compared with wild-type vessels (**C**). Values represent mean ± SEM, the differences in mean was determined by ANOVA. *$p < 0.05$, compared with corresponding control, is considered to be significant.

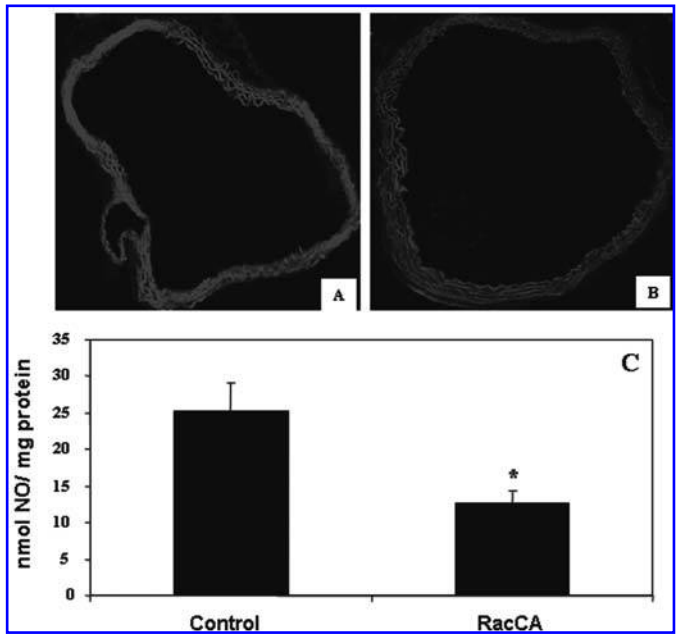

FIG. 4. Decreased NO• levels and metabolites in RacCA aortas. Basal level NO• is assessed in aortic section of RacCA as compared with control mice ($n = 16$) using DAF-2 DA staining in a wild-type aorta (**A**), and NO• level is remarkably decreased in RacCA aorta (**B**). NO• as measured by DAF intensity decreased 59% in RacCA (**C**). Values represent mean ± SEM, *$p < 0.05$.

between young and old transgenic RacCA mice (data not shown). In another experiment, *N*-acetyl-L-cysteine (NAC) was administrated via arterial infusion to RacCA and wild-type mice (0.5 g/kg body weight/day) for 4 days. The administration of NAC resulted in the lowering of blood pressure of both RacCA mice and matched control littermates. The effect of NAC on the MAP of RacCA mice was nearly five times greater than on that of control mice, such that both RacCA and control littermates ended up with a blood pressure averaging 102 mm Hg (Fig. 6C). Discontinuation of NAC caused a return to pre-NAC hypertension in the Rac CA mice (Fig. 6D).

Left ventricular hypertrophy in RacCA mice

Hypertension is commonly associated with left ventricular hypertrophy (LVH). It has been postulated that the development of LVH is secondary to increased work load on the left ventricle created by the excess blood pressure. There was a highly significant increase ($p < 0.0071$) in left ventricular mass in RacCA transgenic mice (112.69 ± 10.9 mg) compared to the control mice (83.35 ± 11.41 mg) (Fig. 7). Similarly, a significant increase was noticed in both posterior (1.087 ± 0.103 mm) and interventricular septal wall thickness (1.095 ± 0.98 mm) in RacCA transgenic mice compared to posterior wall (0.807 ± 0.11 mm) and the septum (0.873 ± 0.23 mm) of the control mice ($p < 0.0071$ for septum and $p < 0.007$ for the posterior wall). There was no significant difference in ejection fraction between RacCA (75 ± 7.1%) and control mice (63 ± 9.5%, $p < 0.21$) nor in the fractional shortening ($p < 0.11$).

DISCUSSION

There is increasing evidence indicating that $O_2^{\bullet -}$ and derived ROS play an important role in the pathophysiology of hypertension. Oxidative stress has been implicated in a variety of hypertensive disorders, including lead-induced hyper-

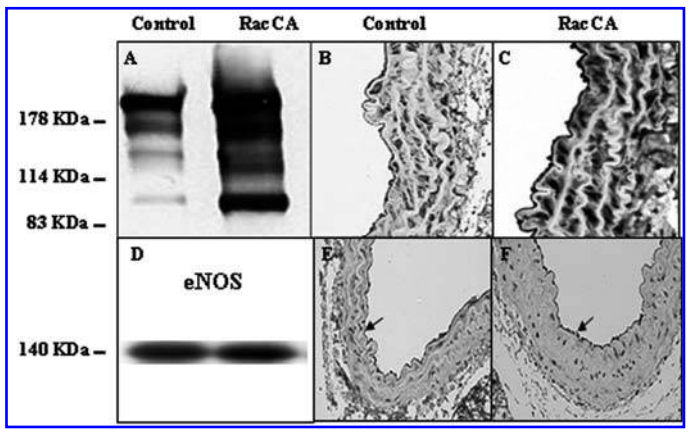

FIG. 5. Increased protein nitration and unaltered eNOS expression in RacCA aortas. Western blot analysis of aortic lysates from Rac CA and matching control mice ($n = 8$), using antinitrotyrosine antibody shows markedly increased protein nitration in RacCA aortas versus wild-type aortic tissues (**A**). Immunohistochemical data obtained in wild-type (**B**) and RacCA aortas (**C**) is consistent with our Western blot finding. Western blot analysis (**D**) and immunohistochemistry in control (**E**) and RacCA transgenic (**F**) aortas using anti-eNOS antibody showed equivalent expression of eNOS.

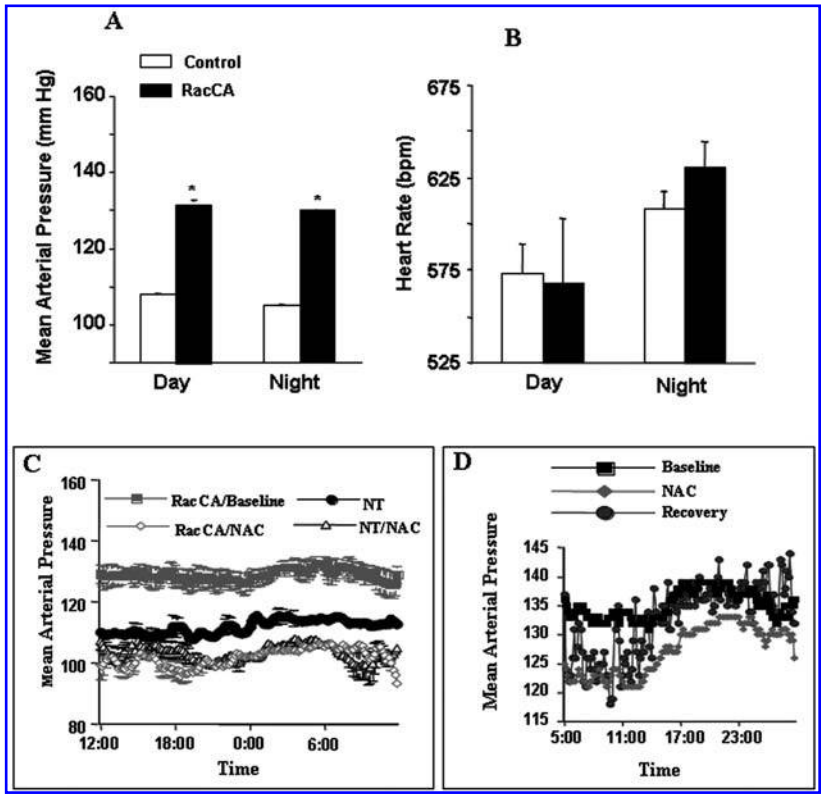

FIG. 6. Circadian blood pressure and heart rate. Continuous monitoring of the mean arterial pressure (MAP ± SEM) via external carotid artery across the night/day cycle of the MAP in transgenic RacCA and matched control littermates mice (n = 8) revealed increased averaged MAP in RacCA as compared with control mice across the night/day cycle (**A**). Continuous monitoring of the heart rate (mean ± SEM) of transgenic RacCA and matched controls (n = 8) mice showed no significant change between RacCA and controls (**B**). The administration of NAC in Rac CA mice (*gray*) and in matched controls (*black*) corrects hypertension in Rac CA mice (**C**). MAP recovers when NAC treatment discontinues (**D**).

tension, uremic hypertension, cyclosporine-induced hypertension, salt-sensitive hypertension, pre-eclampsia, and essential hypertension (24, 29). In Ang II-induced hypertension, rats displayed increased NADPH oxidase activity, expression of p22phox, and ROS levels. NADPH oxidase represents the major source of superoxide and derived ROS (19, 25). Upon binding with GTP, the small GTPase Rac triggers the clustering of NADPH oxidase components, which catalyzes the generation of $O_2^{\bullet -}$ (13, 23). While Rac is capable of activating downstream targets besides NADPH whose role in hypertension also merit attention, perhaps the most unique and conserved function of Rac is its ability to bind to and activate NADPH oxidase complex, which rapidly transfers electrons from NADPH onto molecular oxygen to generate $O_2^{\bullet -}$. Virtually every cell type in the vascular wall has been shown to produce and be regulated by ROS (9). We have demonstrated that ROS are involved in numerous important physiologic responses in cardiovascular biology, probably in concert with other effectors for Rac. For example, efficient migration of endothelial cells requires the generation of $O_2^{\bullet -}$ and derived ROS, a process that involves the uncapping of actin filament barbed ends by oxidants (20). Moreover, we and others have shown that Rac1 is an important stimulator of various aspects of wound healing process via mediating the activation of NADPH oxidase and ROS production (11, 28).

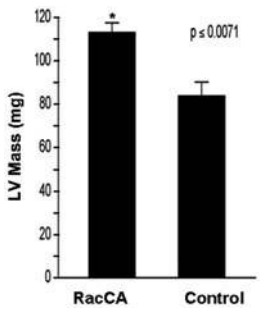

FIG. 7. Echocardiographic study of RacCA mice. Echocardiographic measurement of left ventricular mass was performed on RacCA transgenic (n = 7) and nontransgenic matched controls (n = 7). Data are presented as mean ± SEM. There was significant increases in left ventricular mass in RacCA transgenic mice ($p < 0.0071$).

To characterize the role of Rac activation in vascular biology, we generated a transgenic mouse model overexpressing RacCA selectively in SMCs. We show that the activation of Rac1 in SMCs is sufficient to induce hypertension. The extent of blood pressure elevation (MAP increase of 20–25 mm Hg) is particularly interesting because it is in the range of blood pressure excess seen in humans, and it is equivalent to the blood pressure increase observed in eNOS knockout mice (12). The relevance of our model to the pathophysiology of hypertension is further substantiated by the high level of RacCA expression in aortas and the resultant excessive amounts of $O_2^{\bullet -}$, which interact with $NO^{\bullet}$ to result in increased peroxynitrite formation and reduced NO bioavailability. In addition, Rac-induced hypertension could be corrected by arterial infusion of the antioxidant, NAC, and that the removal of NAC could restore the hypertensive state. The dose of NAC used (0.5 g/Kg body weight/day) was approximately fivefold less than that dose reported in the literature (20 g/L of drinking water/day) (22, 26). In our experience, a low dose of NAC was sufficient to normalize blood if administered via arterial infusion. These data suggest that the Rac-NADPH oxidase pathway may underlie the pathphysiologic changes in

RacCA mice and establish a regulatory effect for Rac in the homeostasis of blood pressure via NADPH oxidase activation and superoxide production.

In this report, we describe that overexpression of a constitutively activated mutant of Rac1, RacCA, in vascular SMCs raises blood pressure without changing the heart rate. There were no significant differences in blood pressure or heart rate between young and old mice (data not shown). The reduction in renin activity observed in RacCA mice could be compensatory response to maintain blood pressure within a normal range. This finding is consistent with the notion that the effect of RacCA on blood pressure is mediated via $O_2^{\bullet -}$ production and perhaps also its interaction with $NO^{\bullet}$.

The cardiac remodeling adaptation to hypertension in RacCA mice consists of left ventricular hypertrophy. The moderate hypertension observed in the RacCA mice is similar to the human pattern. This model enables the evaluation of hypertension secondary to volume overload followed by increased vascular resistance. In addition, the model allows the examination of the LV response to primary changes in the vascular structure and compliance mediated by factors devoid of direct myocardial mitogenic influence.

RacCA overexpression alters the redox balance of the vascular wall. We found increased production of $O_2^{\bullet -}$ via NADPH oxidase, which was suppressed by the specific inhibitor gp91-ds-tat. Heightened $O_2^{\bullet -}$, in turn, interacts with $NO^{\bullet}$ as indicated by increased levels of peroxynitrite in the aortas of transgenic mice. Furthermore, the antioxidant defense mechanisms such as SOD isoforms, catalase, GPX, and GR are upregulated. Despite elevated levels of SOD in the vessels of RacCA mice, these mice are still hypertensive. The increased levels of SOD isoforms in the aortas of Rac CA mice do not appear to be sufficient to inactivate the high levels of free radicals since these are hypertensive mice. It is likely that the high levels of superoxide anions preferably interact and sequester $NO^{\bullet}$. Superoxide anions are known to react rapidly with $NO^{\bullet}$ in solution, with an on-rate of 3.7×10^7 $M^{-1}S^{-1}$ [three times higher than the rate of SOD-catalyzed dismutation (1.2×10^7 $M^{-1}S^{-1}$)] (36). Although both $O_2^{\bullet -}$ and $NO^{\bullet}$ may contribute to the excessive peroxynitrite formation, considering that RacCA aortas exhibit increased $O_2^{\bullet -}$ and decreased $NO^{\bullet}$, it is likely that the elevated levels are primarily responsible for excessive protein nitration in RacCA aortas. Thus, superoxide consumes $NO^{\bullet}$ to form $OONO^-$, thereby disrupting the balance between $NO^{\bullet}$, superoxide anions, and $OONO^-$ to result in predictable changes in vessel tone (hypertension) due to reduction in the availability of $NO^{\bullet}$ at its physiological targets (12). Thus, despite the reduced $NO^{\bullet}$ bioavailability, eNOS expression does not seem to respond, at least at the tissue protein level, to RacCA overexpression. Together, these results suggest that the increased reaction between $O_2^{\bullet -}$ and $NO^{\bullet}$ reduces $NO^{\bullet}$ bioavailability, contributing to the decreased $NO^{\bullet}$ concentration observed in RacCA aortas.

A limitation of the present study is that the analysis of vascular oxidant activity was restricted to the aorta and was not reproduced in resistance arteries. However, the observed changes were consistent with increased activity of Rac1, which would be expected to have similar effects in SMCs cells from proximal and distal arteries. Indeed, the effects of the antioxidant NAC (Fig. 6C and D) suggest that the elevated blood pressure in the RacCA transgenic mice is mediated by increased oxidant activity.

Our unique transgenic model of hypertension provides important biological clues for the pathogenesis of hypertension in the context of Ang II, NADPH oxidase, Rac, $O_2^{\bullet -}$ and $NO^{\bullet}$ Novel therapeutic strategies for the control of blood pressure could be developed and tested on RacCA mice. These findings further underscore the critical importance of the Rac pathway in the cardiovascular system and its pathological settings, such as hypertension and cardiac hypertrophy.

ABBREVIATIONS

DAF-2DA, 4,5-diaminofluorescein diacetate; DETC, diethyldithiocarbamate; DHE, dihyroethidium; DMPO, 5,5′-dimethyl-pyrroline-*N*-oxide; eNOS, endothelial nitric oxide synthase; GPx, glutathione peroxidase; GR, glutathione reductase; NAC, *N*-acetyl-L-cysteine; $NO^{\bullet}$, nitric oxide; $O_2^{\bullet -}$, super oxide; $ONOO^-$, peroxynitrite; Rac 1, small GTP-binding protein of Ras superfamily; RacCA, constitutively active mutant of Rac 1 gene; ROS, reactive oxygen species; SMA, smooth muscle α-actin; SMCs, smooth muscle cells; SODm, superoxide dismutase mimetic.

ACKNOWLEDGMENTS

This work is supported by Grants HL71536 (PJG-C) and HL63744, HL65608 and HL38324 (JLZ) from the National Institutes of Health.

REFERENCES

1. Alpers CE, Seifert RA, Hudkins KL, Johnson RJ, and Bowen–Pope DF. Developmental patterns of PDGF B-chain, PDGF-receptor, and alpha-actin expression in human glomerulogenesis. *Kidney Int* 42: 390–399, 1992.
2. Arnal JF, Dinh–Xuan AT, Pueyo M, Darblade B, and Rami J. Endothelium-derived nitric oxide and vascular physiology and pathology. *J Cell Mol Life Sci* 55: 1078–1087, 1999.
3. Arnal JF, Warin L, and Michel JB. Determinants of aortic cyclic guanosine monophosphate in hypertension induced by chronic inhibition of nitric oxide synthase. *J Clin Invest* 90: 647–652, 1992.
4. Beckman JS and Koppenol WH. Nitric oxide, superoxide, and peroxynitrate: the good, the bad, and the ugly. *Am J Physiol* 271: C1424–C1437, 1996.
5. de Souza H, Laurindo F, Ziegelstein R, Berlowitz C, and Zweier JL. Vascular NAD(P)H oxidase is different from the phagocytic enzyme and is involved in vascular reactivity control. *Am J Physiol* 280: H658–H667, 2001.
6. Garbers LD. The molecular basis of hypertension. *Ann Rev Biochem* 68: 127–155, 1999.
7. Gow AJ, Thom SR, and Ischiropoulos H. Nitric oxide and peroxynitrite-mediated pulmonary cell death. *Lung Cell Mol Phys* 274: L112–L118, 1998.
8. Griendling KK, Minieri D, Ollerenshaw D, and Alexander RW. Angiotensin II stimulates NADH and NADPH oxidase activity in cultured vascular smooth muscle cells. *Circ Res* 74:1141–1148, 1994.
9. Griendling KK, Sorescu D, and Ushio–Fukai M. NAD(P)H oxidase: role in cardiovascular biology and disease. *Circ Res* 86:494–501, 2000.

10. Gulick J, Subramaniam A, Neumann J, and Robbins J. Isolation and characterization of the mouse cardiac myosin heavy chain genes. *J Biol Chem* 266: 9180–9185, 1991.
11. Hassanain H, Irshaid F, Krishna S, Al–kheraije KA, Wisel S, Sheridan J, Michler RE, and Goldschmidt–Clermont PJ. Smooth muscle cell expression of a constitutive active form of human Rac 1 accelerates wound repair. *Surgery* 137: 92–101, 2005.
12. Huang PL, Huang Z, Mashimo H, Bloch KD, Moskowitz MA, Bevan JA, and Fishman MC. Hypertension in mice lacking the gene for endothelial nitric oxide synthase. *Nature* 377: 239–242, 1995.
13. Irani K and Goldschmidt–Clermont PJ. Ras, superoxide and signal transduction. *Biochem Pharmacol* 55: 1339–1346, 1998.
14. Jessup W, Mohr D, and Gieseg SP. The participation of nitric oxide in cell free-and its restriction of macrophage-mediated oxidation of low-density lipoprotein. *Biochem Biophys Acta* 1180: 73–82, 1992.
15. Laufs U, Baeumer, AT, Konkol C, Bohm M, and Nickkenig G. Angiotensin II-induced of Rac1 GTP-binding activity mediates free radicals release and can be inhibited by HMG-CoA reductase inhibitors. American Heart Association meeting. *Circulation* 2: 1479–1485, 2000.
16. Li P, Sur SH, Mistlberger RE, and Morris M. Circadian blood pressure and heart rate rhythms in mice. *Am J Physiol* 276: R500–R504, 1999.
17. Lopes N, Gregg DG, Vasudevan S, Hassanain HH, Goldschmidt–Clermont PJ, and Kovacic H. Feedback by TSP2 regulates cell proliferation induced by Rac 1 redox dependent signaling. *Mol Cell Biol* 23: 5401–5408, 2004.
18. McIntyre M, Bohr DF, and Dominiczak AF. Endothelial function in hypertension: The role of superoxide anion. *Hypertension* 34: 539–545, 1999.
19. Mohazzab KM, Kaminski PM, and Wolin MS. NADH oxidoreductase is a major source of superoxide anion in bovine coronary artery endothelium. *Am J Physiol* 266: H2568–H2572, 1004.
20. Moldovan L, Moldovan NI, Sohn RH, Parikh SA, and Goldschmidt–Clermont PJ. Redox changes of cultured endothelial cells and actin dynamics. *Circ Res* 86: 549–557, 2000.
21. Pardell H, Tresserras R, Armario P, and Hernandez del Rey R. Pharmaco-economic considerations in the management of hypertension. *Drugs* 59: 13–20, 2000.
22. Pechanova O, Zicha J, Kojsova S, Dobesova Z, Jendekova L, Kunes J. Effect of chronic *N*-acetylcysteine treatment on the development of spontaneous hypertension. *Clin Sci* 110: 235–242, 2006.
23. Polakis PG, Weber RF, Nevins B, Didsbury JR, Evans T, and Snyderman R. Identification of the ral and rac1 gene products, low molecular mass GTP-binding proteins from human platelets. *J Biol Chem* 264: 16383–16389, 1989.
24. Raij L. Workshop: hypertension and cardiovascular risk factors: role of the angiotensin II-nitric oxide interaction. *Hypertension* 37: 767–773, 2001.
25. Rajagopalan S, Kurz S, Munzel, T, Tarpey M, Freeman BA, Griendling KK, and Harrison DG. Angiotensin II-mediated hypertension in the rat increases vascular superoxide production via membrane NADH/NADPH oxidase activation: contribution to alteration of vasomotor tone. *J Clin Invest* 97: 1916–1923, 1996.
26. Rauchova H, Pechanova O, Kunes J, Vokurkova M, Dobesova Z, and Zicha J. Chronic *N*-acetylcysteine administration prevents development of hypertension in *N*(omega)-nitro-L-arginine methyl ester-treated rats: the role of reactive oxygen species. *Hypertens Res* 28: 475–482, 2005.
27. Salvemini D, Wang ZQ, Zweier JL, Samouilov A, Macarthur H, Misko TP, Currie MG, Cuzzocrea S, Sikorski JA, and Riley DP. A nonpeptidyl mimic of superoxide dismutase with therapeutic activity in rats. *Science* 286: 304–306, 1999.
28. Sen CK, Khanna S, Babior BM, Hunt TK, Ellison EC, and Roy S. Oxidant-induced vascular endothelial growth factor expression in human keratinocytes and cutaneous wound healing. *J Biol Chem* 277: 33284–33290, 2002.
29. Touyz RM. Oxidative stress and vascular damage in hypertension. *Curr Hypertens Rep* 2: 98–105, 2000.
30. Ushio–Fukai M, Alexander RW, Akers M, Yin Q, Fujio Y, Walsh K, and Griendling KK. Reactive oxygen species mediate the activation of Akt/protein kinase B by angiotensin II in vascular smooth muscle cells. *J Biol Chem* 274: 22699–22704, 1999.
31. Weir MR and Dzau VJ. The renin–angiotensin–aldosterone system: a specific target for hypertension management. *Am J Hypertens* 12: 205S–213S, 1999.
32. Yamazaki J, Fujita N, and Nagao T. NG-Monomethyl-L-arginine-induced repressor response at developmental and established stages in spontaneously hypertensive rats. *J Pharmacol Exp Ther* 259: 52–57, 1991.
33. Yates MT, Lambert LE, and Whitten JP. A protective role for nitric oxide in the oxidative modification of low density lipoproteins by mouse macrophages. *FEBS Lett* 309: 135–138, 1992.
34. Zweier JL. Measurement of superoxide derived free radicals in the reperfused heart: evidence for a free radical mechanism of reperfusion injury. *J Biol Chem* 263:1353–1357, 1988.
35. Zweier JL, Broderick R, Kuppusamy P, Thompson–Gorman S, and Lutty GA. Determination of the mechanism of free radical generation in human aortic endothelial cells exposed to anoxia and reoxygenation. *J Biol Chem* 269: 24156–24162, 1994.
36. Zweier JL, Kuppusamy P, Williams R, Rayburn BK, Smith D, Weisfeldt ML, and Flaherty JT. Measurement and characterization of postischemic free radical generation in the isolated perfused heart. *J Biol Chem* 264: 18890–18895, 1989.

Address reprint requests to:
Hamdy H. Hassanain
Department of Anesthesiology and Dorothy
M. Davis Heart and Lung Research Institute
473 West 12th Avenue
Columbus OH 43210

E-mail: hamdy.hassanain@osumc.edu

Date of first submission to ARS Central, August 30, 2006; date of final revised submission, August 30, 2006; date of acceptance, August 31, 2006.

This article has been cited by:

1. Elisabeth M. Storck, Beata Wojciak-Stothard. 2012. Rho GTPases in pulmonary vascular dysfunction. *Vascular Pharmacology* . [CrossRef]
2. Hagen Maxeiner, Yaser Abdallah, Christoph Rüdiger Wolfram Kuhlmann, Klaus-Dieter Schlüter, Sibylle Wenzel. 2012. Effects of cerivastatin on adrenergic pathways, hypertrophic growth and TGFbeta expression in adult ventricular cardiomyocytes. *European Journal of Cell Biology* . [CrossRef]
3. Colin E. Murdoch, Sara P. Alom-Ruiz, Minshu Wang, Min Zhang, Simon Walker, Bin Yu, Alison Brewer, Ajay M. Shah. 2011. Role of endothelial Nox2 NADPH oxidase in angiotensin II-induced hypertension and vasomotor dysfunction. *Basic Research in Cardiology* **106**:4, 527-538. [CrossRef]
4. Henning Morawietz. 2011. Endothelial NADPH oxidases: friends or foes?. *Basic Research in Cardiology* **106**:4, 521-525. [CrossRef]
5. Jongyun Heo . 2011. Redox Control of GTPases: From Molecular Mechanisms to Functional Significance in Health and Disease. *Antioxidants & Redox Signaling* **14**:4, 689-724. [Abstract] [Full Text HTML] [Full Text PDF] [Full Text PDF with Links]
6. Gervaise Loirand, Pierre Pacaud. 2010. The role of Rho protein signaling in hypertension. *Nature Reviews Cardiology* **7**:11, 637-647. [CrossRef]
7. Ryan J Sullivan, Liron Pantanowitz, Bruce J Dezube. 2009. Studying Rac1-induced tumorigenesis suggests antioxidants may help prevent and treat Kaposi's sarcoma. *Future Oncology* **5**:7, 949-952. [CrossRef]
8. Q. Ma, L. E. Cavallin, B. Yan, S. Zhu, E. M. Duran, H. Wang, L. P. Hale, C. Dong, E. Cesarman, E. A. Mesri, P. J. Goldschmidt-Clermont. 2009. Antitumorigenesis of antioxidants in a transgenic Rac1 model of Kaposi's sarcoma. *Proceedings of the National Academy of Sciences* **106**:21, 8683-8688. [CrossRef]
9. Abel Martin Garrido, Kathy K. Griendling. 2009. NADPH oxidases and angiotensin II receptor signaling. *Molecular and Cellular Endocrinology* **302**:2, 148-158. [CrossRef]
10. L. MYATT, R. P. WEBSTER. 2009. Vascular biology of preeclampsia. *Journal of Thrombosis and Haemostasis* **7**:3, 375-384. [CrossRef]
11. Ravi Nistala , Adam Whaley-Connell , James R. Sowers . 2008. Redox Control of Renal Function and Hypertension. *Antioxidants & Redox Signaling* **10**:12, 2047-2089. [Abstract] [Full Text HTML] [Full Text PDF] [Full Text PDF with Links]
12. M Oka, K A Fagan, P L Jones, I F McMurtry. 2008. Therapeutic potential of RhoA/Rho kinase inhibitors in pulmonary hypertension. *British Journal of Pharmacology* **155**:4, 444-454. [CrossRef]
13. Moo Yeol Lee , Kathy K. Griendling . 2008. Redox Signaling, Vascular Function, and Hypertension. *Antioxidants & Redox Signaling* **10**:6, 1045-1059. [Abstract] [Full Text HTML] [Full Text PDF] [Full Text PDF with Links]
14. Y BIAN, Y QI, Z YAN, D LONG, B SHEN, Z JIANG. 2008. A proteomic analysis of aorta from spontaneously hypertensive rat: RhoGDI alpha upregulation by angiotensin II via AT1 receptor. *European Journal of Cell Biology* **87**:2, 101-110. [CrossRef]